PPPL-3226, Preprint: January 1997, UC-426

Local tests of parallel electrical resistivity in the Tokamak Fusion Test Reactor

S. H. Batha and F. M. Levinton
Fusion Physics and Technology, Inc.
3547 Voyager Street, Torrance CA 90503-1673

A. T. Ramsey, G. L. Schmidt, and M. C. Zarnstorff
Princeton Plasma Physics Laboratory
Princeton, NJ 08543

The motional Stark effect (MSE) polarimeter measures the local magnetic field pitch angle, proportional to the ratio of the poloidal to toroidal magnetic fields, in the Tokamak Fusion Test Reactor (TFTR). We have used the polarimeter to measure the temporal evolution of the local value of the magnetic field pitch angle during large changes in the current profile such as during a current ramp or discharge initiation. The measured evolution is compared to the evolution predicted by classical and neoclassical resistivity models. The neoclassical resistivity model is a better predictor of the local pitch angle temporal evolution than the classical model.

PACS Numbers: 52.30.Bt, 52.55.-s

I. Introduction

Determination of the correct model of plasma resistivity is crucial for understanding current tokamak discharges and for the design of future tokamak devices such as ITER. In this work, two models are considered. Classical or Spitzer resistivity[1] is predicted for a plasma embedded in a uniform magnetic field. Neoclassical resistivity[2,3] extends classical theory to include electron trapping corrections in an axisymmetric toroidal plasma. These trapping corrections imply the existence of the bootstrap current,[4] a phenomenon where the plasma generates a portion of its own toroidal current by diffusion of trapped electrons parallel to the magnetic field. Fine control of the bootstrap current profile is assumed in the design of advanced tokamaks and other steady-state devices and reactors.[5]

Resistivity measurements at many tokamaks and other plasma devices have been summarized by Zarnstorff *et al.*[6] and by Kaye *et al.*[7] The results have been mixed. Broadly, better agreement with classical resistivity has been found for small- and medium-sized devices while larger (and hotter) devices have found better agreement with neoclassical theory. There are exceptions to this generalization, however. For example, Kaye *et al.* found mixed results on the PBX-M tokamak.[7] Some discharges were better fit by the classical model, while other discharges departed significantly from either model. Early PDX results indicated better agreement with classical at low toroidal field but better agreement with neoclassical at higher field.[8] Recent results from Alcator-C-Mod indicate a resistivity between the classical and neoclassical results.[9] On the Tokamak Fusion Test Reactor (TFTR),[10] the surface voltage calculated using neoclassical resistivity was in much better agreement with experimental measurements in Ohmic plasmas over a wide range of plasma conditions than was the classical calculation.[6] Neoclassical resistivity was also consistent with recent measurements on Tore Supra.[11]

In this paper, the results of a series of experiments on TFTR are presented where large changes were induced in the current-density profile by a decrease in the total plasma current (a current "ramp down") or during the "start up" phase of a discharge when the

current is penetrating to the center of the plasma. The main experimental result is the time-resolved measurement of the magnetic field pitch profile, $\gamma_p = \arctan(B_{pol}/B_{tor})$, where B_{pol} and B_{tor} are the poloidal and toroidal magnetic fields, respectively.

The pitch angle is measured by the motional Stark effect (MSE) diagnostic from the polarized emission of neutral-beam atoms in the strong magnetic field of the tokamak.[12,13] Several improvements in diagnostic techniques allow a unique set of data to be brought to bear on the resistivity question. When most of these measurements were made, the MSE diagnostic on TFTR consisted of a ten channel device with sightlines between major radii, R, of 2.51 to 3.45 m. The MSE coverage was from inside the magnetic axis to the outer edge of the plasma. The diagnostic measures local pitch information across the minor radius of the plasma and so is an internal measurement.[14] Previous analysis of plasmas from TFTR[6] and other devices concentrated on Ohmic discharges to test the resistivity models against global measurements of the plasma surface voltage. Experiments on PBX-M[7] used a moveable, single-point MSE diagnostic to compile a pitch-angle profile, at a single time, during a sequence of Ohmic or neutral-beam-heated discharges. In the experiments presented here, the internal pitch-angle profile was measured continuously for 2 seconds in low-power, neutral-beam-heated plasmas. Internal measurements have also been made recently on DIII-D and TEXT-Upgrade. Neoclassical resistivity was inferred from equilibrium reconstructions based on MSE measurements on DIII-D.[15] Classical resistivity has been inferred from equilibrium reconstructions using far-infrared polarimetry measurements on TEXT-Upgrade.[16]

The design of the experiments is presented in section II. The temporal evolution of the pitch angles during and after a current ramp down is compared with the models in section III. Measurements of current penetration during discharge start up are presented in section IV and compared to model predictions.

II. Experimental Design

The discharge start up and current ramp down experiments were performed immediately after the multichannel MSE diagnostic was installed on TFTR. The absolute calibration of the instrument, at that time, was uncertain. Since then, techniques have been developed to decrease the uncertainty in the absolute calibration.[17,18] One consequence of calibration uncertainty is that equilibrium codes are not able to reconstruct either the q or current-density profile with confidence for the measurements presented in this paper. Due to the uncertainty in the value of the measured profile, plasma conditions were designed which would cause large relative changes in the pitch angle profiles, such as current ramps and during discharge start up. The uncertainty in the relative change at each local point is small, being determined almost solely by statistical noise. Therefore, the results of this paper do not depend on the absolute calibration of the MSE diagnostic.

The measured pitch-angle evolution for each experiment is compared with the predictions of a fully time-dependent code, TRANSP.[19] Measured density profiles from a ten-channel far-infrared polarimeter,[20] electron temperature profiles from an electron cyclotron emission (ECE) radiometer,[21] and the central or profile[22] Z_{eff} are used to determine self-consistently the kinetic pressure profile and the magnetically measured shape and location of the outermost flux surface. The fast-ion pressure due to neutral beam injection is modeled using a Monte Carlo technique.[23] TRANSP numerically solves the poloidal diffusion equation in toroidal coordinates and calculates the poloidal flux as a function of time. The precise form of the poloidal diffusion equation, and of the classical and neoclassical resistivities used by TRANSP, are given in reference 6, whose notation is followed in this paper. TRANSP may employ either classical, neoclassical, or alternative resistivity models in its calculation. TRANSP may also use a sawtooth model based on the Kadomtsev current mixing model. Results using the Kadomtsev model show no substantial differences from the neoclassical model predictions and will not be discussed in this paper.

III. Current Ramp Down

Large, rapid changes of the plasma current while keeping the plasma major radius constant cause large changes in the pitch angles which increase the sensitivity of the simulations to the resistivity model employed. Parameters from such a discharge are displayed in figure 1. An $I_p = 2.0$ MA, $R = 2.45$ m plasma had reached steady state before the 9 MW of neutral beam power was injected at 3.0 sec. The plasma current was decreased to 1.0 MA between 3.5 sec and 4.0 sec with a constant current ramp rate of -2.0 MA/sec. The surface voltage became negative as soon as the current ramp down began and remained negative for the duration of neutral beam injection.

The evolution of the pitch angles at $R = 2.83$ m and 2.92 m is shown in figures 2(a) and 2(c), respectively. For all sightlines, there was virtually no change in the pitch angles before the current ramp, from 3.0 to 3.5 sec. During the current ramp, all of the pitch angles decreased due to an outward shift of the magnetic axis. At the end of the current ramp, the pitch angle stopped changing for $R \leq 2.83$ m [*e.g.* figure 2(a)], but continued to decrease for $R \geq 2.92$ m [*e.g.* figure 2(c)]. The change during the current ramp ranges from 0.8° (at 2.51 m) to 2.5° (at 3.24 m).

The MSE measurement can be polluted by large radial electric fields, E_r, in the plasma.[24] The MSE data may be corrected by computing E_r from the radial force balance equation using a post-processor to TRANSP, calculating the correction, and then applying it to the data. The correction is a offset to the data that changes in time and radius. The calculated correction for these experiments is small but improves the match between the measurements and predictions significantly. Data presented in this paper includes the effects of E_r and represents a change of -0.15° in figures 2(a) and 2(c) from the beginning of the discharge to the end, no change in figure 6, and changes of about +0.12° in figures 7(a) and 7(c).

For each MSE sightline, the neoclassical model reproduces the data better than the classical resistivity model. The neoclassical predictions, however, are not within the uncertainty of the measurements. For $R \leq 2.83$ m, the classical model predicts a smaller change in pitch angle than actually measured so that the predicted pitch angle may be larger than measured by up to +0.6° [figure 2(b)]. The neoclassical predictions are a factor of 2 closer to the measured data than the classical prediction, but may still be up to +0.2° too large. For $R \geq 2.92$ m, the classical model predicts either that the pitch angle stops evolving after the current ramp ends (2.92 m $\leq R \leq$ 3.00 m) [figure 2(d)], or a smaller change than measured ($R \geq 3.00$ m). For $R \geq 3.00$ m, the classical prediction may be as much as 1.0° larger than measured while the neoclassical prediction may be as much as 0.3° larger.

The effective charge of the plasma, Z_{eff}, is an important parameter in determining the resistivity evolution. Two different assumptions about the radial structure of Z_{eff} have been used in analyzing TFTR discharges. The first assumption is that the value of Z_{eff} is constant across the diameter of the plasma and is derived from a single radial measurement of the visible bremsstrahlung emissivity.[22] The second assumption is that Z_{eff} has radial structure inferred from the visible bremsstrahlung emissivity measured by a tangentially viewing array of detectors normalized to the single-channel radial measurement. The inferred Z_{eff} profile for the discharge shown in figs. 1 and 2 is shown in fig. 3(a). The value of Z_{eff} near the edges is slightly higher, and the central value slightly lower, than the constant-Z_{eff} assumption. The inferred resistivity profile, fig. 3(b), and calculated q profile, fig. 3(c), from the neoclassical model change only slightly when using radially varying Z_{eff} compared to the constant Z_{eff} result. The classical resistivity is much different than either of the neoclassical calculations. Inclusion of a radially varying Z_{eff} makes a small correction to the calculated pitch angle evolution for both resistivity models and is used for all model predictions used in this paper.

The simulations also calculate the q profile, fig. 3(c), under the various resistivity assumptions. The neoclassical simulation predicts that q(0), the central safety factor, is about 0.7, which is much more realistic than the classical prediction of 1.3. The neoclassical pitch angle profile is also closer to the profile predicted by the equilibrium code[25] VMEC which solves the MHD force-balance equation constrained by external magnetics, internal kinetic, and MSE data. The VMEC equilibria find that $q(0) \approx 0.8$. Because the MSE data is not absolutely calibrated, complete reliance on the equilibrium code results is not warranted. However, the results are indicative of the true equilibrium and are supporting evidence for the preference of the neoclassical model to describe this discharge.

As well as uncertainty in the measurements, there is uncertainty in the model predictions. These are the result of uncertainties in the experimental data used by TRANSP to determine the resistivity and consequently, the poloidal field and magnetic field pitch angle. To quantify these errors, a series of 30 TRANSP runs were made with the important experimental data varied within their uncertainties. The electron density profile[20] had an uncertainty of less than $\pm 1.5 \times 10^{12}$ cm^{-3}, the electron temperature[21] determined by ECE was assumed to have a one standard deviation uncertainty of 4%, and the value of Z_{eff} had an uncertainty of 10%. A spatially invariant Z_{eff} was assumed in all of the TRANSP runs used in the uncertainty analysis.

Figure 4 shows that the neoclassical evolution calculated using the nominal experimental data has no significant difference from the average of the 30 TRANSP calculations. The neoclassical value is also a good match to the measured data within the error bars of the calculation during the ramp down and until about 4.5 sec. After that, the calculation deviates from the measurement until it is three standard deviations away from the data at the end of the pulse. The uncertainty in the relative value of the MSE data is only 0.06° at the end of the pulse, so there is no overlap of the uncertainties of the measurement and calculation. One possible explanation of the discrepancy is that TRANSP is

not calculating the correct magnetic axis. TRANSP calculates a magnetic axis that is 6 cm outboard of the peak in the electron density and temperature profiles at 4.75 sec. A shift of the pitch angle profile by this distance would bring the prediction into agreement with the measurement at that time. The discrepancy in axis location begins to appear at about 4 sec and would explain the appearance of the "knee" in the neoclassical calculation at that time.

IV. Current Penetration at the Beginning of a Discharge

The tokamak plasmas studied for the discharge start up portion of this experiment had plasma currents at steady state, I_p, of 1.0, 1.4, and 1.8 MA and were heated by 4.5 MW of balanced, tangential neutral-beam injection. The evolution of the global parameters are shown in figure 5. Neutral beam injection and MSE measurements began at about 1.5 sec and lasted for 2 seconds. Neutral beam injection began before the plasma current reached the programmed value. It was impossible, at the time of this experiment, to inject the neutral beam any earlier because of power supply limitations and plasma density control interlocks. Also, MSE measurements would have been affected by a varying toroidal field if measurements had been attempted earlier since the toroidal field did not reach full field until 1.5 sec. It should be noted that $\beta_{pol} < 0.36$ for all the discharges studied in this section, thus minimizing any bootstrap currents.

The discharges at I_p = 1.0 and 1.4 MA had energy confinement times less than predicted by Goldston L-mode scaling.[26] Sawteeth began at about 2.25 sec in each discharge. There was no other significant MHD activity. The 1.8 MA discharges also had sawteeth, beginning at 1.5 sec. Again, there was no other significant MHD activity. The 1.8 MA discharges had energy confinement times which rose from L-mode at 1.5 sec to about twice L-mode by 3.5 sec.

The pitch angle evolution at two fixed major radii are shown in figures 6 and 7 for the I_p = 1.0 and 1.8 MA discharges, respectively. Figures 6(a) and 7(a) show the data and

model predictions for R = 2.62 m, about 0.05 m inside the magnetic axis, while figures 6(c) and 7(c) display the data for R = 2.92 m.

The discharges at I_p = 1.0 and 1.4 MA evolved the same way. The plasma was "grown" from the outer limiter so that the geometric axis was at a major radius of 2.59 m at 1.5 sec and reached the final value of 2.56 m at 1.9 sec. The behavior of the pitch angle at each MSE sightline for $R \leq 2.73$ is approximately the same: The measured data showed a rapid decrease and then increase between 1.5 and 1.8 sec followed by an evolution of less than 0.1° during the remainder of the measurement [figure 6(a)]. A small decrease of less than 0.2° until 1.7 sec followed by a monotonic increase until the end of the measurement was seen at each sightline for 2.83 m $\leq R \leq$ 3.24 [figure 6(c)]. The increase was strictly monotonic for $R \geq$ 3.00 m. At 1.4 MA, the increase was strictly monotonic for $R \geq$ 2.83 m.

Direct comparisons among the two models and the measurements for the I_p = 1.0 MA case are made in figures 6(b) and 6(d) where the difference between the TRANSP calculations and the data are shown. There are no substantial differences among the two models and the data for the R = 2.62 m data shown in figure 6(a). At R = 2.92 m, the pitch angle was measured to change by more than +0.7°. In figure 6(d) it can be seen that the classical prediction underestimates the change by 0.2° while the difference between the neoclassical prediction and the data is always less than 0.1°. This level is consistent with the statistical noise of the MSE measurement.[17] The classical prediction is consistently low by almost 0.2°, which is less than the expected uncertainty in the relative calibration at R = 2.92 m.

The pitch angle temporal evolution was very different for the I_p = 1.8 MA case as shown in figure 7. Part of this change was due to a different discharge formation scenario. The plasma current reached its final value later, compared to the 1.0 MA case (see figure 5), and the plasma current ramp rate was much faster for the 1.8 MA case. Also, the plasma began at a smaller radius (2.1 m) and its size was increased while the current was

increasing which caused faster penetration of the current to the center of the plasma. This was just the opposite of the 1.0 and 1.4 MA plasmas.

For $R \leq 2.83$ m, the pitch angle decreased by one to two degrees between 1.5 and 2.0 sec and then only decreased slightly for the duration of the measurement [see figure 7(a)]. For $R \geq 2.92$ m, the pitch angle decreased by 0.5° to 0.0° in less than 0.5 sec, and then increased monotonically after 2.0 sec. The maximum change in the measured pitch angle was approximately +1.3° at $R = 3.09$ m. Comparison of the data with the models is made more explicit in figure 7. At $R = 2.62$ m in figures 7(a) and 7(b), the neoclassical model tends to predict a larger change than measured by underestimating the pitch angle by up to 0.4°. The classical model predicts too little change in pitch angle and so overestimates the pitch angle by up to 0.6°. The uncertainty in the relative change is estimated to be less than ±0.1°. At larger major radii, such as $R = 2.92$ m in figures 7(c) and 7(d), the classical model predicts no change after 2.0 sec while the data shows a change of +0.8°. The neoclassical model is much closer to the data and predicts a change of +0.7° after 2.0 sec, but has overestimated the decrease between 1.5 and 2.0 sec.

V. Conclusion

Local, internal, time-resolved measurements of the magnetic field pitch angle using motional-Stark-effect polarimetry were made in low-power neutral-beam-heated discharges in TFTR. It was found that the neoclassical resistivity model was a better description of current penetration than was the classical resistivity model. It is obvious from an analysis of figures 2, 6, and 7, and from the rest of the data which are not shown, that neither the neoclassical nor the classical model correctly predicts the pitch angle evolution during either the current penetration phase of discharge start up or during a rapid current decrease to within the accuracy that this evolution can be measured. However, the calculation using the neoclassical model was always in better agreement than the classical (Spitzer)

calculation. In most cases, particularly in the outer half of the plasma, the classical model was grossly incorrect while the neoclassical calculation was within 2 standard deviations of the measurement. Both models had difficulty in the core of the plasma.

Acknowledgments

The authors would like to thank Z. Chang for data on MHD activity, J. Felt for software support, R. E. Bell for analysis of CHERS data, and S. M. Kaye for useful discussions on resistivity studies. This work was supported by the U. S. Department of Energy Contract No. DE-AC02-76-CH03073.

References

1. L. Spitzer and R. Harm, *Phys. Rev.* **89**, 977 (1953).

2. S. P. Hirshman and D. J. Sigmar, *Nucl. Fusion* **21**, 1079 (1981).

3. F. L. Hinton and R. D. Hazeltine, *Rev. Mod. Phys.* **48**, 239 (1976).

4. R. J. Bickerton, J. W. Connor, and J. B. Taylor, *Nature* **229**, 110 (1971).

5. R. J. Goldston, S. H. Batha, R. H. Bulmer, D. N. Hill, A. W. Hyatt, S. C. Jardin, F. M. Levinton, S. M. Kaye, C. E. Kessel, E. A. Lazarus, J. Manickam, G. H. Neilson, W. M. Nevins, L. J. Perkins, G. Rewoldt, K. I. Thomassen, M. C. Zarnstorff, and N. T. Team, *Plasma Physics and Controll. Fusion* **36**, B213 (1994).

6. M. C. Zarnstorff, K. McGuire, M. G. Bell, B. Grek, D. Johnson, D. McCune, H. Park, A. Ramsey, and G. Taylor, *Phys. Fluids B* **2**, 1852 (1990).

7. S. M. Kaye, F. M. Levinton, R. Hatcher, R. Kaita, C. Kessel, B. LeBlanc, D. C. McCune, and S. Paul, *Phys. Fluids B* **4**, 651 (1992).

8. S. Kaye, R. Goldston, M. Bell, K. Bol, M. Bitter, R. Fonck, B. Grek, R. Hawryluk, D. Johnson, R. Kaita, H. Kugel, D. Mansfield, D. McCune, K. McGuire, D. Mueller, M. Okabayashi, D. Owens, G. Schmidt, and P. Thomas, *Nucl. Fusion* **24**, 1303 (1984).

9. M. Greenwald, R. L. Boivin, P. Bonoli, C. Christensen, C. Fiore, D. Garnier, J. Goetz, S. Golovato, M. Graf, R. Granetz, S. Horne, T. Hsu, A. Hubbard, I. Hutchinson, J. Irby, C. Kurz, B. LaBombard, B. Lipschultz, T. Luke, E. Marmar, G. McCracken, A. Niemczewski, P. O'Shea, M. Porkolab, J. Rice, J. Reardon, J. Schacter, J. Snipes, P. Stek, Y. Takase, J. Terry, M. Umansky, R. Watterson, and S. Wolfe, *Phys. Plasmas* **2**, 2308 (1995).

10. R. J. Hawryluk, V. Arunasalam, M. G. Bell, M. Bitter, W. R. Blanchard, N. L. Bretz, R. Budny, C. E. Bush, J. D. Callen, S. A. Cohen, S. K. Combs, S. L. Davis, D. L. Dimock, H. F. Dylla, P. C. Efthimion, L. C. Emerson, A. C. England, H. P. Eubank, R. J. Fonck, E. Fredrickson, H. P. Furth, G. Gammel, R. J. Goldston, B. Grek, L. R. Grisham, G. Hammett, W. W. Heidbrink, H. W. Hendel, K. W. Hill, E. Hinnov, S. Hiroe, R. A. Hulse, H. Hsuan, K. P. Jaehnig, D. Jassby, F. C. Jobes, D. W. Johnson, L. C. Johnson, R. Kaita, J. Kamperschroer, S. M. Kaye, S. J. Kilpatrick, R. J. Knize, H. Kugel, P. H. LaMarche, B. LeBlanc, R. Little, C. H. Ma, D. M. Manos, D. K. Mansfield, M. P. McCarthy, R. T.

McCann, D. C. McCune, K. McGuire, D. H. McNeill, D. M. Meade, S. S. Medley, D. R. Mikkelsen, S. L. Milora, W. Morris, D. Mueller, V. Mukhovatov, E. B. Nieschmidt, J. O'Rourke, D. K. Owens, H. Park, N. Pomphrey, B. Prichard, A. T. Ramsey, M. H. Redi, A. L. Roquemore, P. H. Rutherford, N. R. Sauthoff, G. Schilling, J. Schivell, G. L. Schmidt, S. D. Scott, S. Sesnic, J. C. Sinnis, F. J. Stauffer, B. C. Stratton, G. D. Tait, G. Taylor, J. R. Timberlake, H. H. Towner, M. Ulrickson, V. Vershkov, S. v. Goeler, F. Wagner, R. Wieland, J. B. Wilgen, M. Williams, K. L. Wong, S. Yoshikawa, R. Yoshino, K. M. Young, M. C. Zarnstorff, V. S. Zaveriaev, and S. J. Zweben, in *Plasma Physics and Controlled Nuclear Fusion Research, Proceedings of the 11th International Conference, Kyoto, 1986*, (International Atomic Energy Agency, Vienna, 1987), Vol. I, pp. 51.

11. E. Joffrin, B. Saoutic, V. Basiuk, C. Forest, W. A. Houlberg, T. Hutter, C. E. Kessel, and X. Litaudon, 22nd European Physics Conference on Controlled Fusion and Plasma Physics, Bournemouth, Great Britain (European Physics Society, Petit-Lancy, Switzerland, 1995), Part. IV, p. 125.

12. F. M. Levinton, *Rev. Sci. Instrum.* **63**, 5157 (1992).

13. F. M. Levinton, R. J. Fonck, G. M. Gammel, R. Kaita, H. W. Kugel, E. T. Powell, and D. W. Roberts, *Phys. Rev. Lett.* **63**, 2060 (1989).

14. S. H. Batha, F. M. Levinton, and M. C. Zarnstorff, *Bull. Am. Phys. Soc.* **39**, 1676 (1994).

15. C. B. Forest, K. Kupfer, T. C. Luce, P. A. Politzer, L. L. Lao, M. R. Wade, D. G. Whyte, and D. Wroblewski, *Phys. Rev. Lett.* **73**, 2444 (1994).

16. D. L. Brower, Y. Jiang, L. Zeng, G. Cima, H. Gasquet, J. Lierzer, P. E. Phillips, B. W. Rice, D. R. Roberts, D. C. Sing, R. Steimle, and A. J. Wootton, 22nd European Physics Conference on Controlled Fusion and Plasma Physics, Bournemouth, Great Britain (European Physics Society, Petit-Lancy, Switzerland, 1995), Part. IV, p. 129.

17. F. M. Levinton, S. H. Batha, M. Yamada, and M. C. Zarnstorff, *Phys. Fluids B* **5**, 2554 (1993).

18. F. M. Levinton, S. H. Batha, and M. C. Zarnstorff, *to be published in Rev. Sci. Instrum.* (1997).

19. R. J. Hawryluk, Proc. of the Course on Physics of Plasma Close to Thermonuclear Conditions, Brussels (CEC, 1980), Part. p. 19.

20. H. K. Park, *Rev. Sci. Instrum.* **61**, 2879 (1990).

21. G. Taylor, P. Efthimion, M. McCarthy, V. Arunasalam, R. Bitzer, J. Bryer, R. Cutler, E. Fredd, M. A. Goldman, and D. Kaufman, *Rev. Sci. Instrum.* **55**, 1739 (1984).

22. A. T. Ramsey and S. L. Turner, *Rev. Sci. Instrum.* **58**, 1211 (1987).

23. R. J. Goldston, D. C. McCune, H. H. Towner, S. L. Davis, R. J. Hawryluk, and G. L. Schmidt, *J. Comp. Phys.* **43**, 61 (1981).

24. M. C. Zarnstorff, F. M. Levinton, S. H. Batha, and E. J. Synakowski, *submitted to Phys. Plasmas* (1996).

25. S. P. Hirshman, D. K. Lee, F. M. Levinton, S. H. Batha, M. Okabayashi, and R. M. Wieland, *Phys. Plasmas* **1**, 2277 (1994).

26. R. J. Goldston, *Plasma Phys. and Cont. Fusion* **26**, 87 (1984).

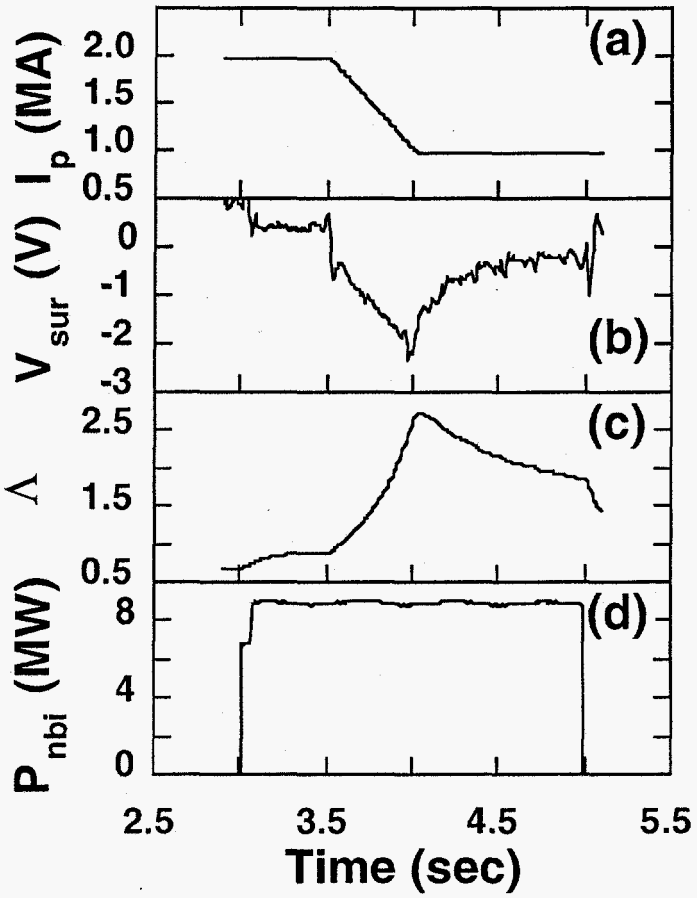

Figure 1. Time evolution of plasma current I_p, surface voltage V_{sur}, $\Lambda \equiv \beta_{pol} + \ell_i/2$, and neutral beam heating power P_{nbi}, for a discharge with a -2.0 MA/sec current ramp at 3.5 sec. The plasma major radius was $R = 2.45$ m.

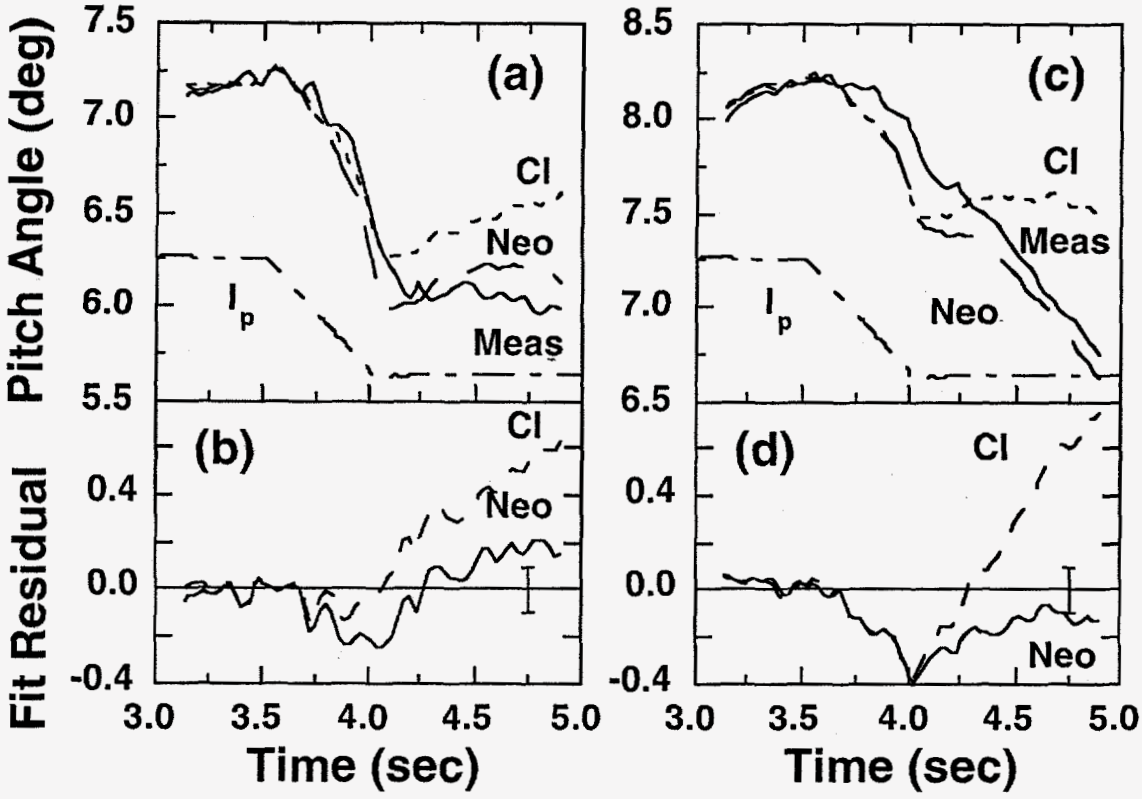

Figure 2. The measured pitch angle evolution (solid line) at (a) R = 2.83 m and (c) R = 2.92 m for a discharge with a current ramp from 2 to 1 MA between 3.5 and 4.0 sec. The neoclassical (long dash) and classical (short dash) predictions are shown. The difference between the measured pitch angles and the TRANSP calculations using neoclassical (solid) and classical (dashed) resistivity models are shown in (c) and (d), respectively. A positive number means that the model is predicting a larger pitch angle than measured. The MSE data and the classical prediction have been normalized to the neoclassical calculation for the time interval 3.13 sec to 3.49 sec by adding a constant offset angle.

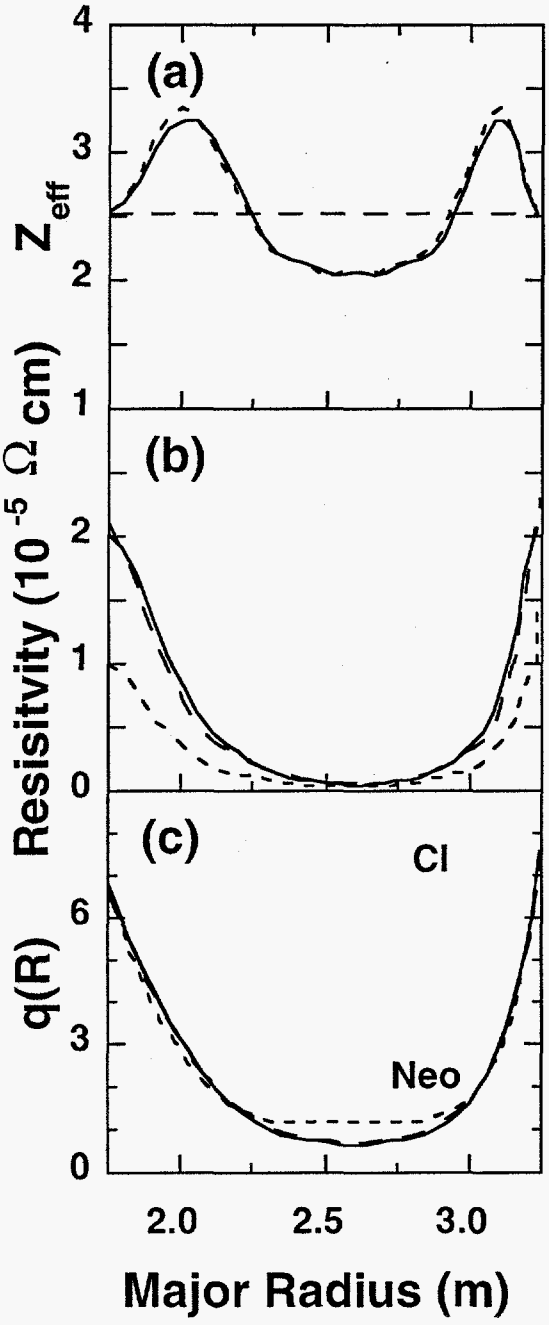

Figure 3. Three interpretations of the (a) Z_{eff} profile at 4.75 sec for the discharge shown in fig. 1. The (b) resistivity and (c) q profiles were calculated assuming either neoclassical or classical resistivity and the different $Z_{eff}(R)$ profile. Shown are neoclassical calculations from either a constant $Z_{eff}(R)$ (long dashed line) or a spatially varying $Z_{eff}(R)$ (solid line). Also shown is the classical calculation from a spatially varying $Z_{eff}(R)$ (short dashed line).

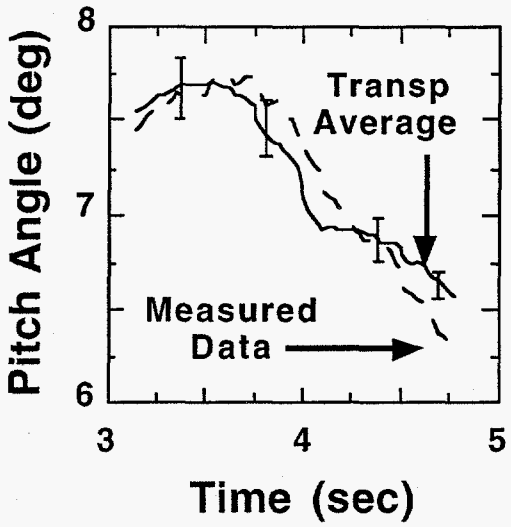

Figure 4. The uncertainty of the TRANSP analysis of a discharge similar to that shown in figs. 1 and 2 at $R = 2.92$ m using the neoclassical resistivity model. The measured electron temperature and density profiles and the experimental value of Z_{eff} were varied by their experimental uncertainty before TRANSP calculated the pitch angle evolution. Shown are the measured data (dashed line), and the average of the 30 TRANSP calculations (solid line). The nominal neoclassical calculation is indistinguishable from the average. The error bars represent the $\pm 1\ \sigma$ standard deviation of the TRANSP runs. The MSE data has been offset to agree with the averaged neoclassical pitch angle between 3.40 and 3.66 sec.

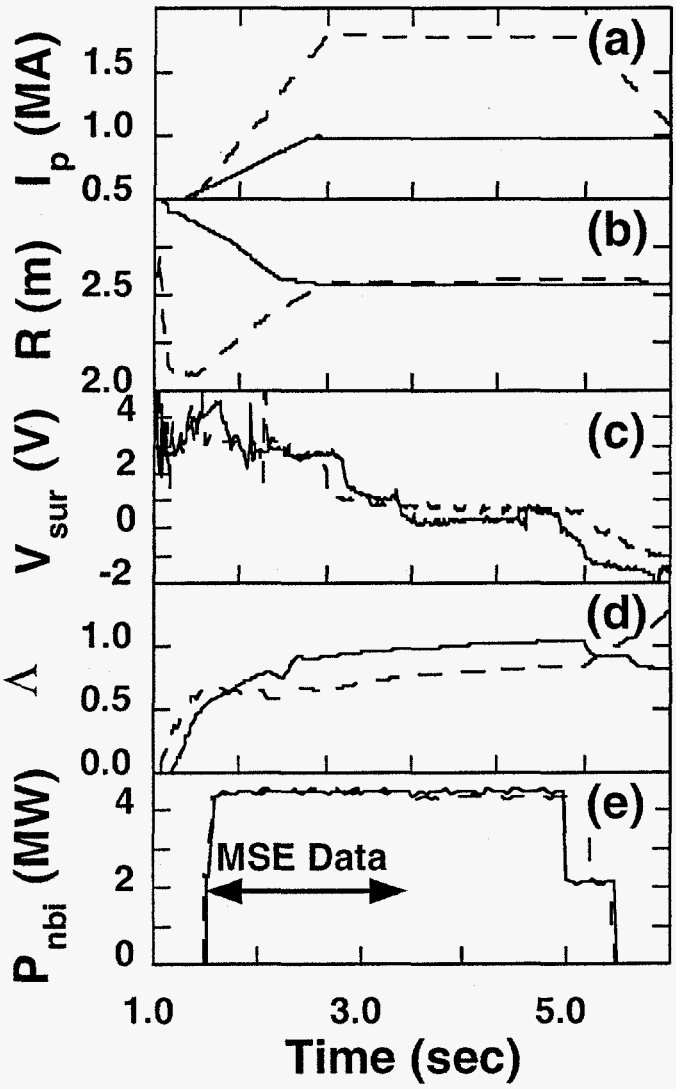

Figure 5. Time evolution of plasma current I_p, major radius R, $\Lambda \equiv \beta_{pol} + \ell_i/2$, surface voltage V_{sur}, and neutral beam heating power P_{nbi}, for two discharges with different plasma currents.

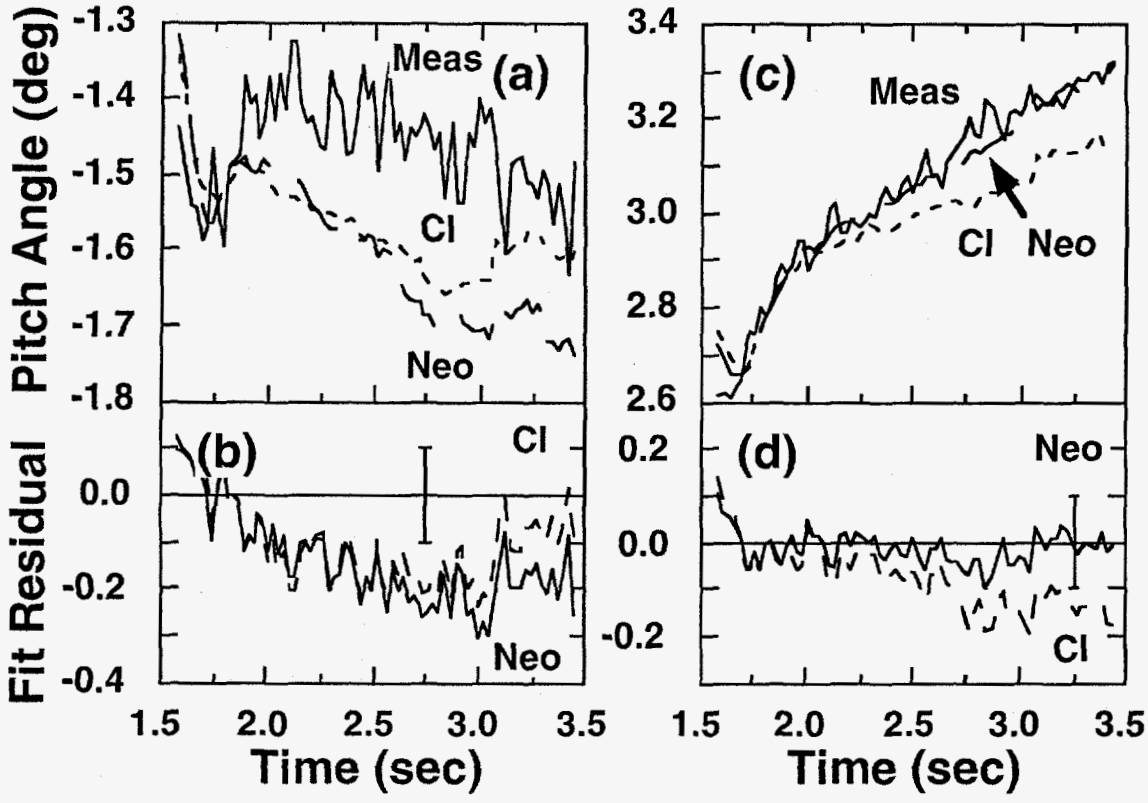

Figure 6. The measured pitch angle evolution (solid line) at (a) R = 2.62 m and (c) R = 2.92 m for an I_p = 1.0 MA discharge. The neoclassical (long dash) and classical (short dash) predictions are shown. The difference between the measured pitch angles and the TRANSP calculations using neoclassical (solid) and classical (dashed) resistivity models are shown in (c) and (d), respectively. A positive number means that the model is predicting a larger pitch angle than measured. The MSE data and the classical prediction have been normalized to the neoclassical calculation for the time interval 1.58 sec to 1.98 sec by adding a constant offset angle.

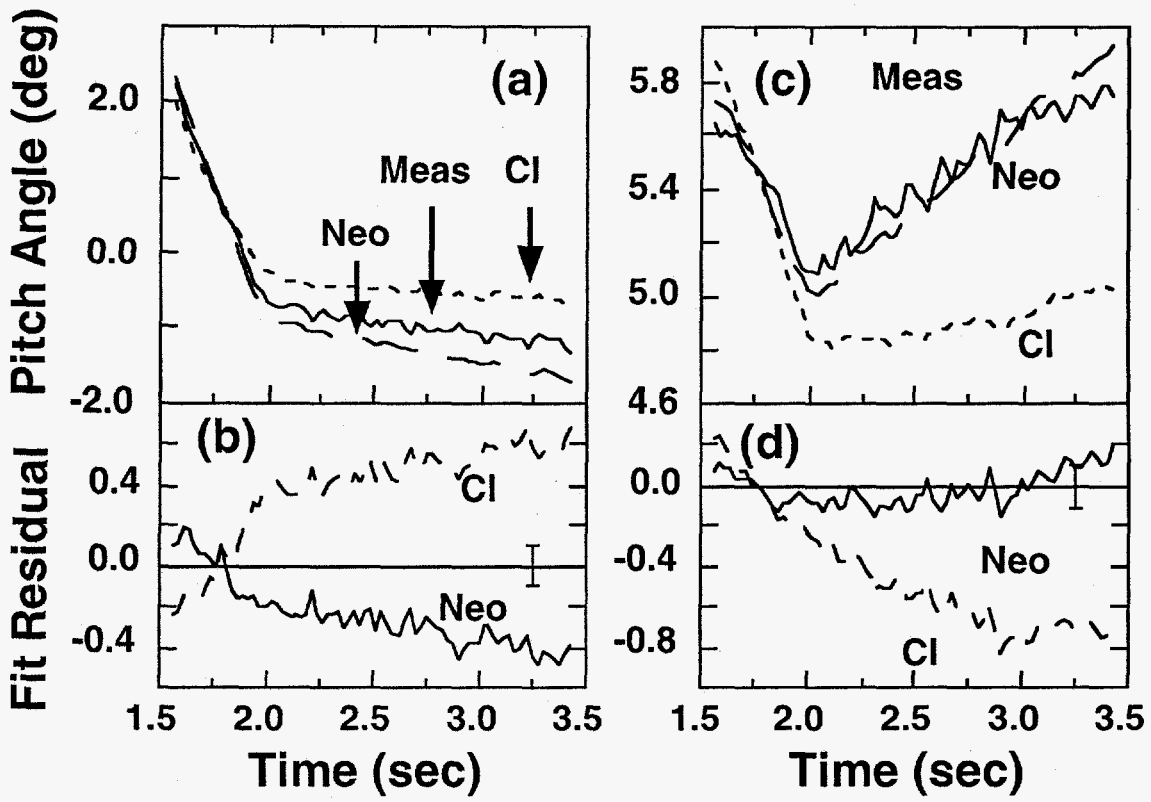

Figure 7. The measured pitch angle evolution (solid line) at (a) $R = 2.62$ m and (c) $R = 2.92$ m for an $I_p = 1.8$ MA discharge. The neoclassical (long dash) and classical (short dash) predictions are shown. The difference between the measured pitch angles and the TRANSP calculations using neoclassical (solid) and classical (dashed) resistivity models are shown in (c) and (d), respectively. A positive number means that the model is predicting a larger pitch angle than measured. The MSE data and the classical prediction have been normalized to the neoclassical calculation for the time interval 1.56 sec to 1.96 sec by adding a constant offset angle.